

Supporting Information

An Unprecedented Oxidised Julolidine-BODIPY Conjugate and its Application in Real-time Ratiometric Fluorescence Sensing of Sulfite

D. Sirbu, L. Zeng, P. G. Waddell and A. C. Benniston

Table of Contents

Figure S1. ^1H NMR spectrum for OXJUL in DMSO- d_6	3
Figure S2. ^{11}B NMR spectrum for OXJUL in DMSO- d_6	3
Figure S3. ^{19}F NMR spectrum for OXJUL in DMSO- d_6	4
Figure S4. Mass spectrum for OXJUL showing the $[\text{M}]^+$ ion.....	4
Figure S5. Selected bond lengths and angles for JUL and OXJUL in DMSO solvent using IEF-PCM model calculated at B3PW91/6-311+G(d, p) theoretical level.....	5
Figure S6. Absorption spectrum for JUL in DMSO and its deconvolution into a series of Guassian bands.....	6
Figure S7. Absorption spectrum for OXJUL in DMSO and its deconvolution into a series of Guassian bands.....	7
Figure S8. Ground-state DFT calculated frontier MO energy changes for JUL and OXJUL in DMSO solvent using IEF-PCM model at B3PW91/6-311+G(d, p) theoretical level.....	8
Figure S9. UV-Vis-NIR absorption spectra for compounds of JUL (blue) and OXJUL (red) in DMSO: experimental values (a) and DFT calculated using IEF-PCM solvent model at B3PW91/6-311+G(d, p) theoretical level (b).....	9
Figure S10. Curly arrow mechanisms showing the sites of hydrogensulfite anion attachment to the BODIPY core.....	10
Figure S11. Top: Partial 700 MHz ^1H NMR spectra of OXJUL in d_6 -DMSO before (A) and after (B) the addition of Na_2SO_3 (aq) showing selected resonances and their shifts. A sample left for one week showing loss of the proton signal for 7 (C) and the alteration in the spectrum upon addition of a small amount of acid (D). Bottom: Calculated chemical shifts for the proposed sulfite addition product with the corresponding measured chemical shifts in red. Note: the upfield shift for proton 6 suggests that electron density is slightly increased at the site, consistent with the decrease in electron-withdrawing nature of the julolidine group.....	11
Figure S12. ^1H NMR spectra collected for OXJUL in d_6 -DMSO before and after the addition of acid (B & C) plus a comparison with the spectrum recorded one week after the addition of Na_2SO_3 in the presence of acid (A). Lines indicate resonances not observed between the two samples and it is noted the difference in broadness of the resonances.....	12

Figure S13. Fluorescence changes observed for dilute DMSO solutions of OXJUL upon the addition of Na ₂ SO ₃ (aq) and the proposed chemical reactions.....	13
Figure S14. An APPI mass spectrum collected from a solution of OXJUL in DMSO after the addition of Na ₂ SO ₃ (aq).....	14
Figure S15. Changes to the absorption spectra for an aqueous solution of OXJUL (pH 7) after the addition of Na ₂ SO ₃ (aq) with the insert showing the isosbestic point. The red line indicates the excitation wavelength used for the fluorescence experiments and the slight increase in the optical density as the reaction proceeds.....	15
Figure S16. Kinetic plots showing the alterations in I(634)/I(580) versus time for several different equivalents of sulphite. Table of calculated rate constants.....	16
Figure S17. Calibration plots at various times for the detection of sulfite by OXJUL (conc = 0.47 μM).....	17
Figure S18. Anion selectivity comparison using the emission intensity ratio I ₅₉₀ /I ₆₄₅ for OXJUL upon addition of (a) F ⁻ (b) Cl ⁻ (c) Br ⁻ (d) I ⁻ (e) SO ₃ ²⁻ (f) SO ₄ ²⁻ (g) PO ₄ ³⁻ (h) NO ₃ ⁻ (i) NO ₂ ⁻ (j) CO ₃ ²⁻ (k) CH ₃ COO ⁻ (3.9×10^{-4} mmol, $\lambda_{\text{ex}} = 525$ nm) in EtOH / H ₂ O (75 %, v/v).....	18
Figure S19. (a) UV-Vis absorption spectra of the iodometric measurement for sulfite detection upon different [SO ₃ ²⁻] after reacting with I ₂ . (b) The linear correlation plot for the UV-Vis absorption at 569 nm vs different [SO ₃ ²⁻].....	19
Figure S20. An example of UV-Vis absorbance changes during an iodometric measurement for a dry white wine sample.....	20
Table S1. Crystal data and structure refinement details for OXJUL	21
Table S2. Results from DFT Calculations.....	22

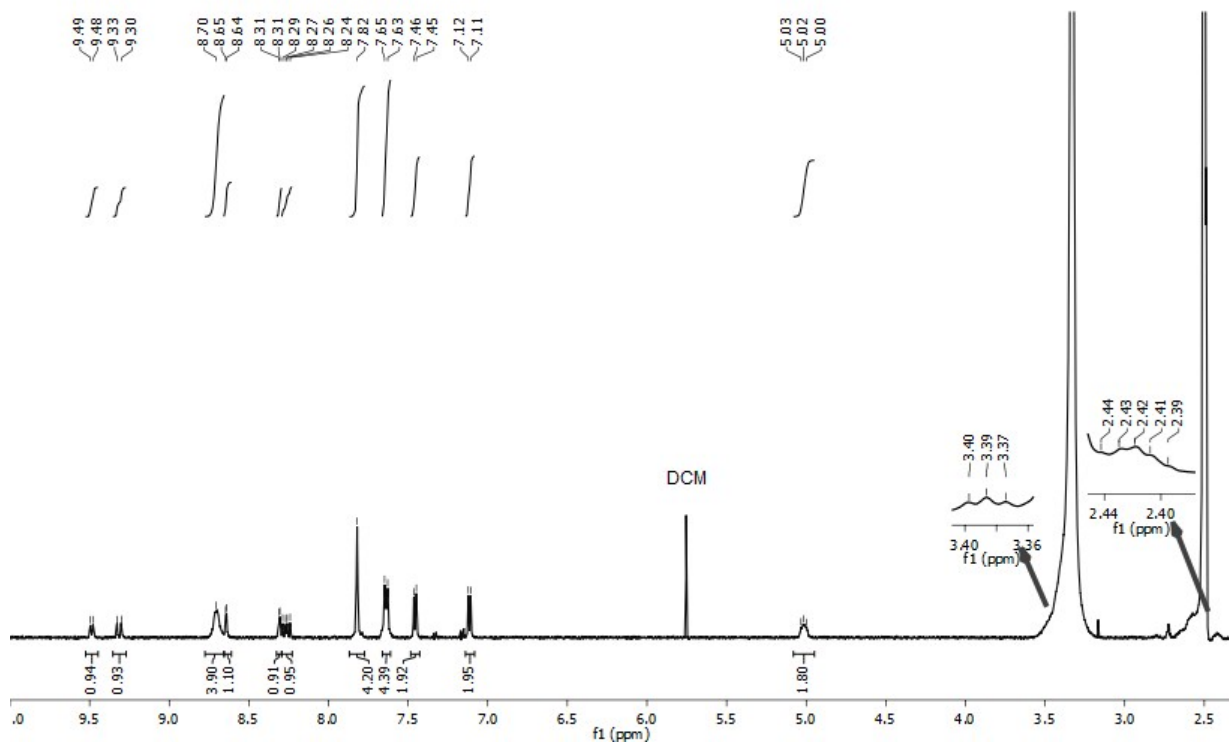


Figure S1. ^1H NMR spectrum for OXJUL in $\text{DMSO}-d_6$.

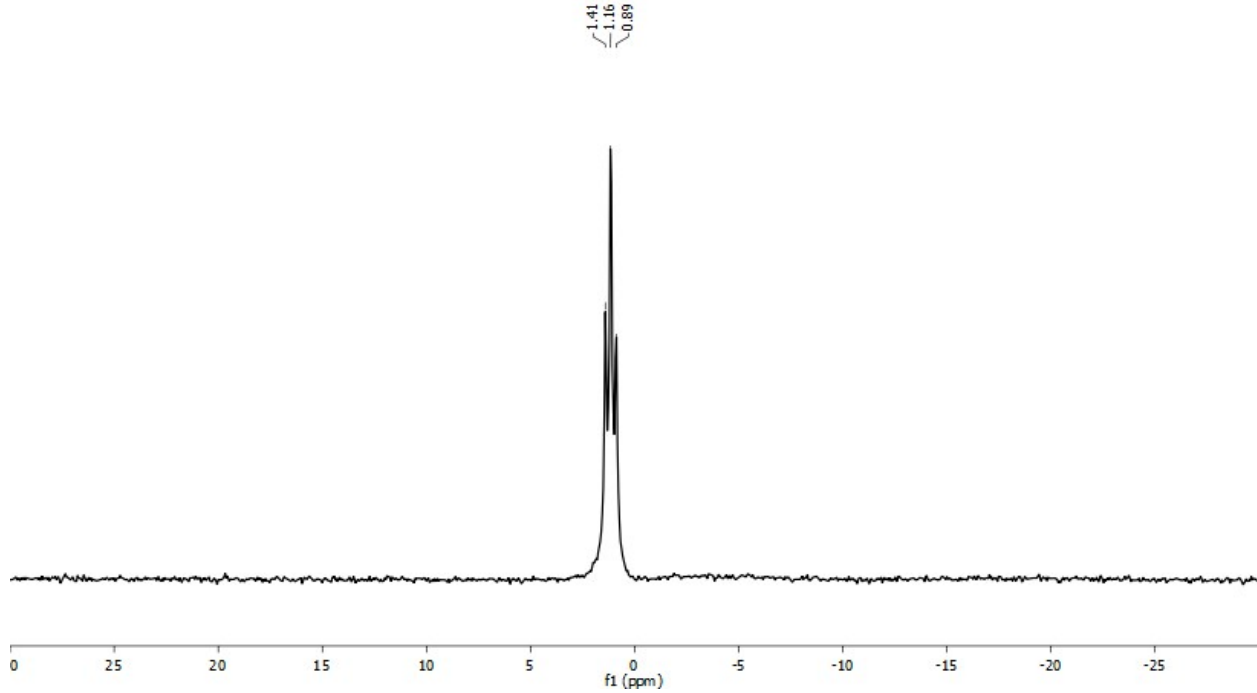


Figure S2. ^{11}B NMR spectrum for **OXJUL** in $\text{DMSO}-d_6$.

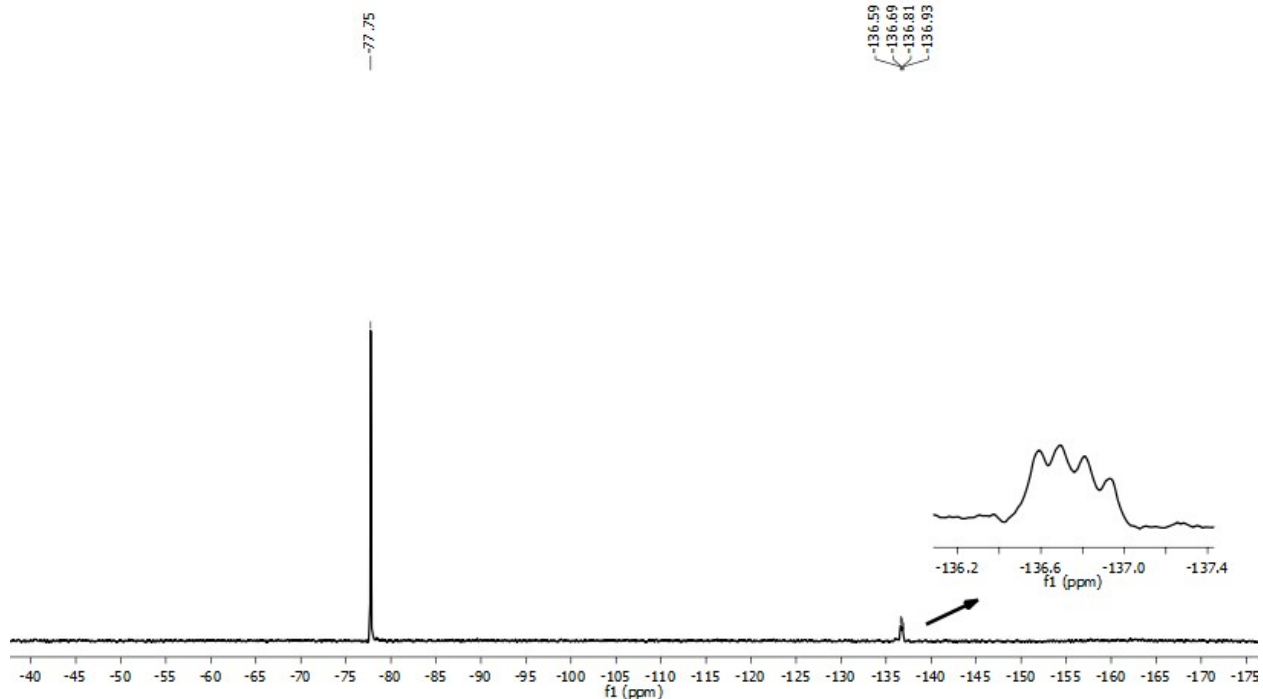


Figure S3. ^{19}F NMR spectrum for **OXJUL** in $\text{DMSO}-d_6$.



Figure S4. Mass spectrum for **OXJUL** showing the $[\text{M}]^+$ ion.

Atoms	JULBD2	^{ox}JULBD2
B – F ^a	1.410 Å	1.408
N – B ^a	1.544 Å	1.548
C = C ^a _{trans}	1.350 Å	1.350
F – B – F	108.48 °	108.91
N – B – N	107.65 °	107.38
JUL – BD ^b	45.0 °	60.8

^aAverage of the two bonds length. ^bThe angle formed by BODIPY and julolidine planes.

Figure S5. Selected bond lengths and angles for **JUL** and **OXJUL** in DMSO solvent using IEF-PCM model calculated at B3PW91/6-311+G(d, p) theoretical level.

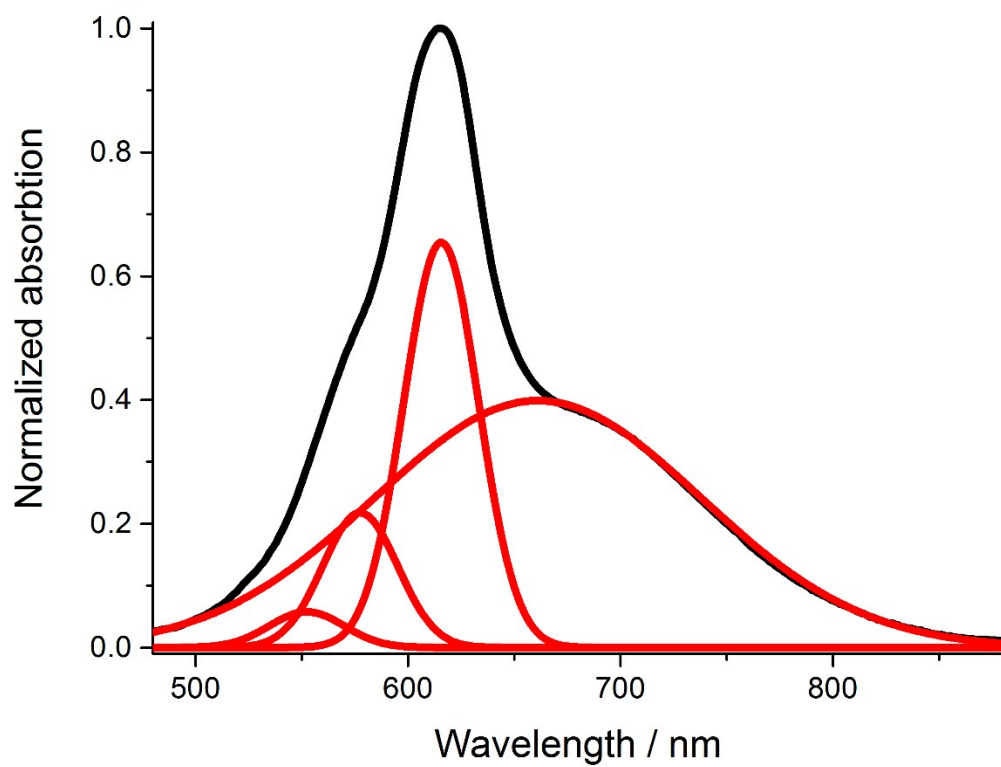


Figure S6. Absorption spectrum for **JUL** in DMSO and its deconvolution into a series of Gaussian bands.

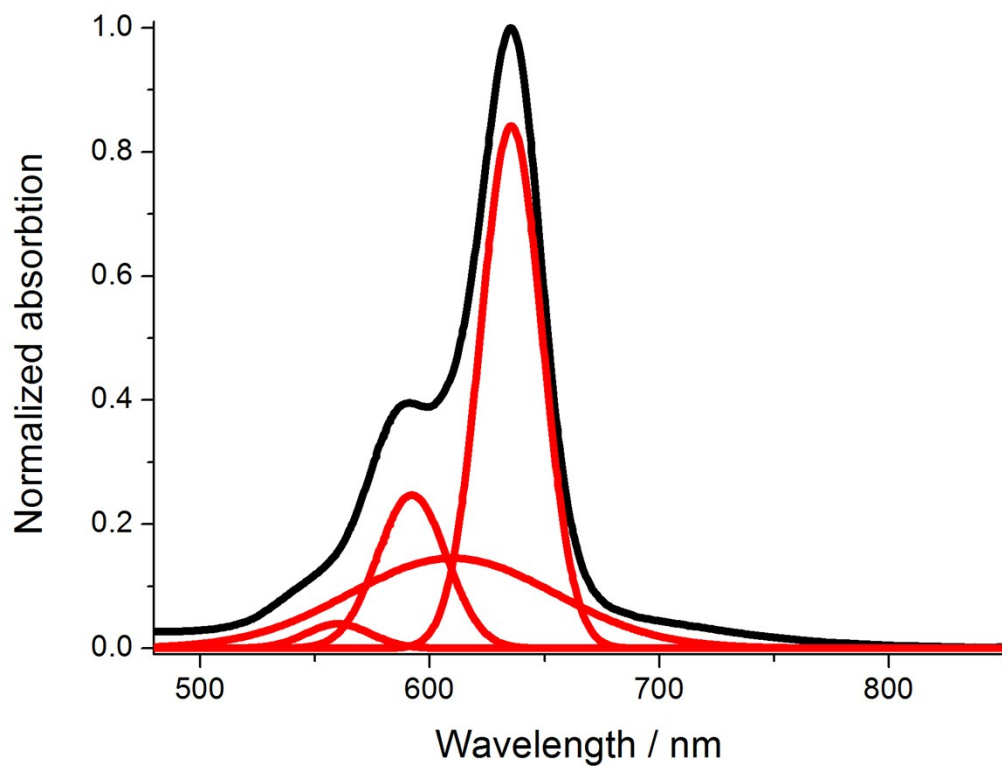


Figure S7. Absorption spectrum for **OXJUL** in DMSO and its deconvolution into a series of Gaussian bands.

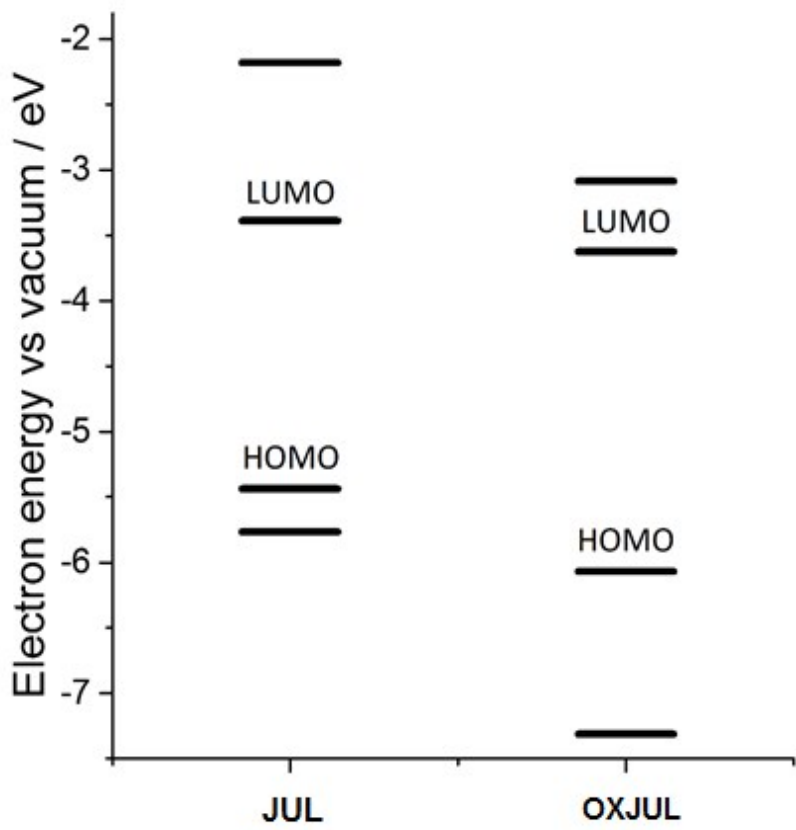


Figure S8. Ground-state DFT calculated frontier MO energy changes for **JUL** and **OXJUL** in DMSO solvent using IEF-PCM model at B3PW91/6-311+G(d, p) theoretical level.

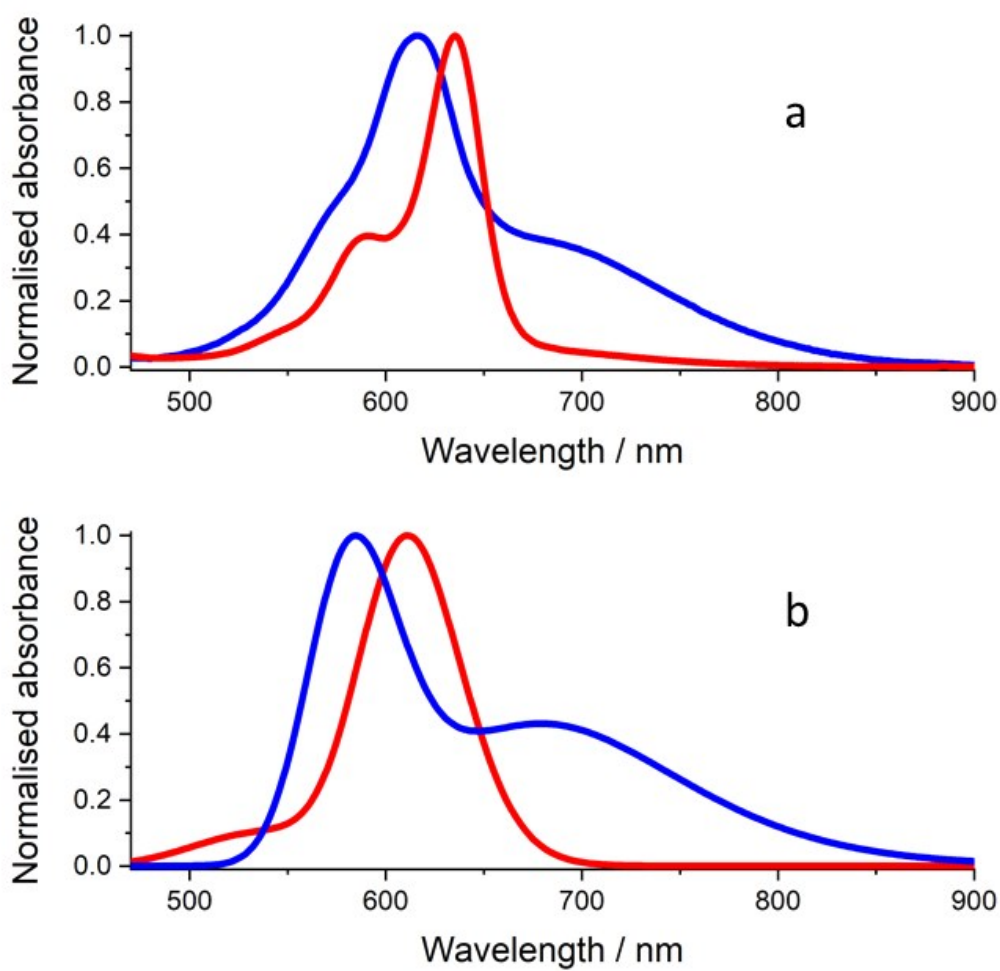


Figure S9. UV-Vis-NIR absorption spectra for compounds of **JUL** (blue) and **OXJUL** (red) in DMSO: experimental values (a) and DFT calculated using IEF-PCM solvent model at B3PW91/6-311+G(d, p) theoretical level (b).

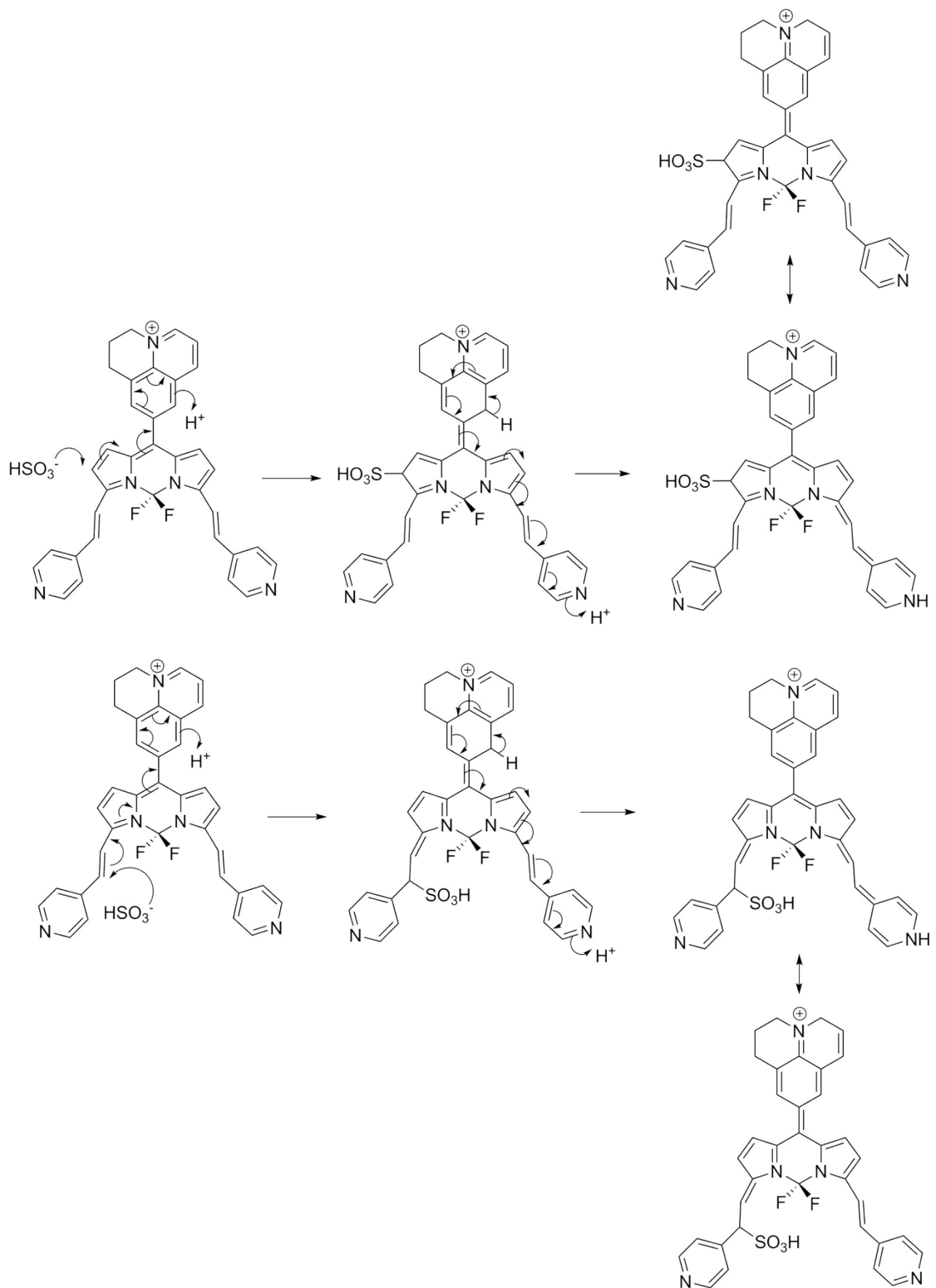


Figure S10. Curly arrow mechanisms showing the sites of hydrogensulfite anion attachment to the BODIPY core.

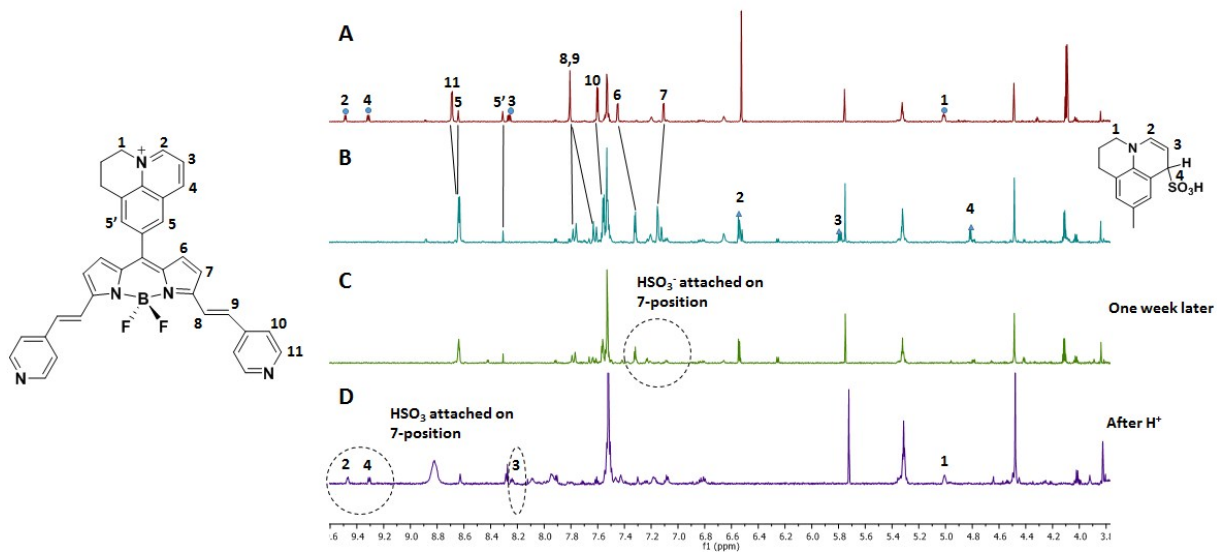


Figure S11. Top: Partial 700 MHz ¹H NMR spectra of **OXJUL** in d₆-DMSO before (**A**) and after (**B**) the addition of Na₂SO₃ (aq) showing selected resonances and their shifts. A sample left for one week showing loss of the proton signal for **7** (**C**) and the alteration in the spectrum upon addition of a small amount of acid (**D**). Bottom: Calculated chemical shifts for the proposed sulfite addition product with the corresponding measured chemical shifts in red. Note: the upfield shift for proton **6** suggests that electron density is slightly increased at the site, consistent with the decrease in electron-withdrawing nature of the julolidine group.

A: Sample left for one week (with acid)

B: Original sample

C: Addition of acid

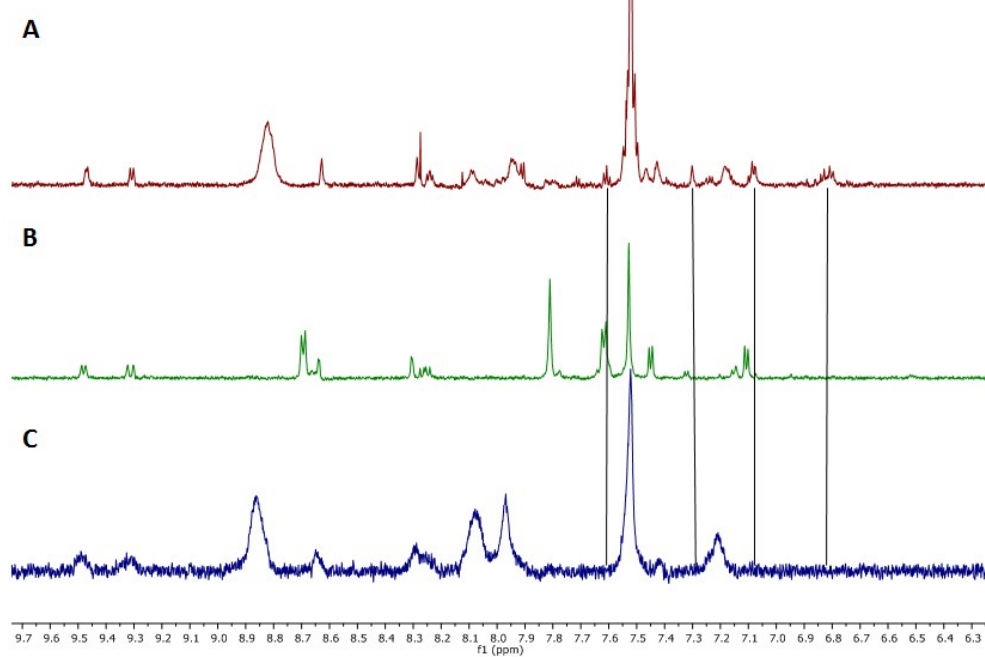


Figure S12. ¹H NMR spectra collected for **OXJUL** in d₆-DMSO before and after the addition of acid (B & C) plus a comparison with the spectrum recorded one week after the addition of Na₂SO₃ in the presence of acid (A). Lines indicate resonances not observed between the two samples and it is noted the difference in broadness of the resonances.

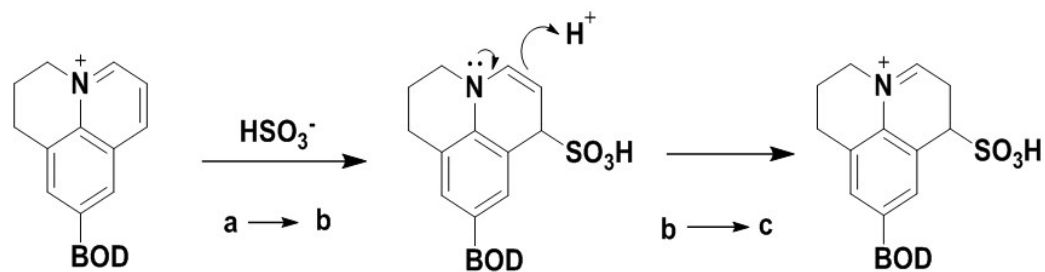
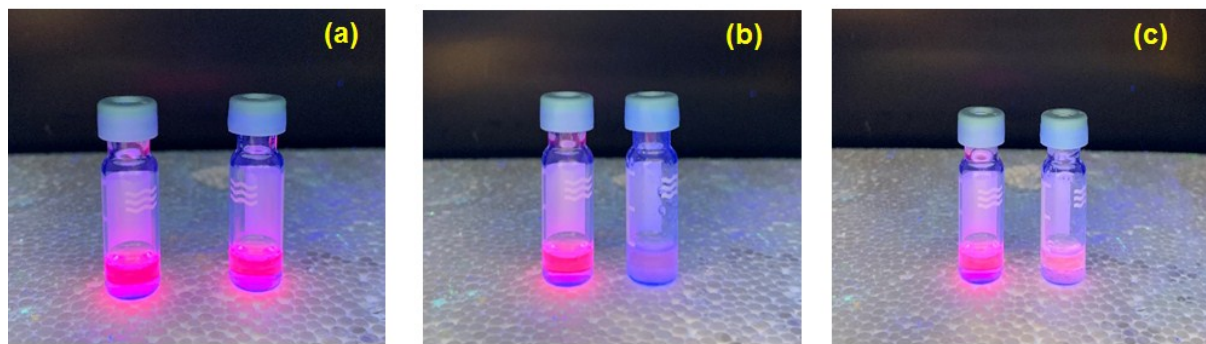


Figure S13. Fluorescence changes observed for dilute DMSO solutions of **OXJUL** upon the addition of Na₂SO₃ (aq) and the proposed chemical reactions.

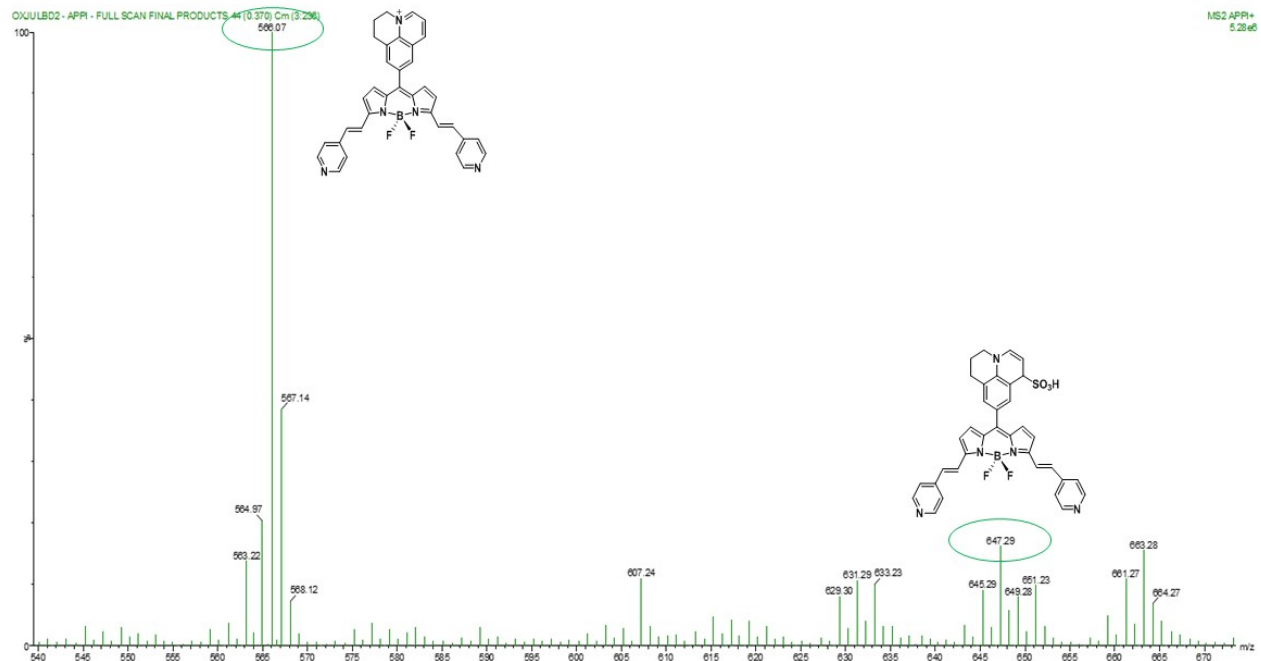


Figure S14. An APPI mass spectrum collected from a solution of **OXJUL** in DMSO after the addition of Na_2SO_3 (aq).

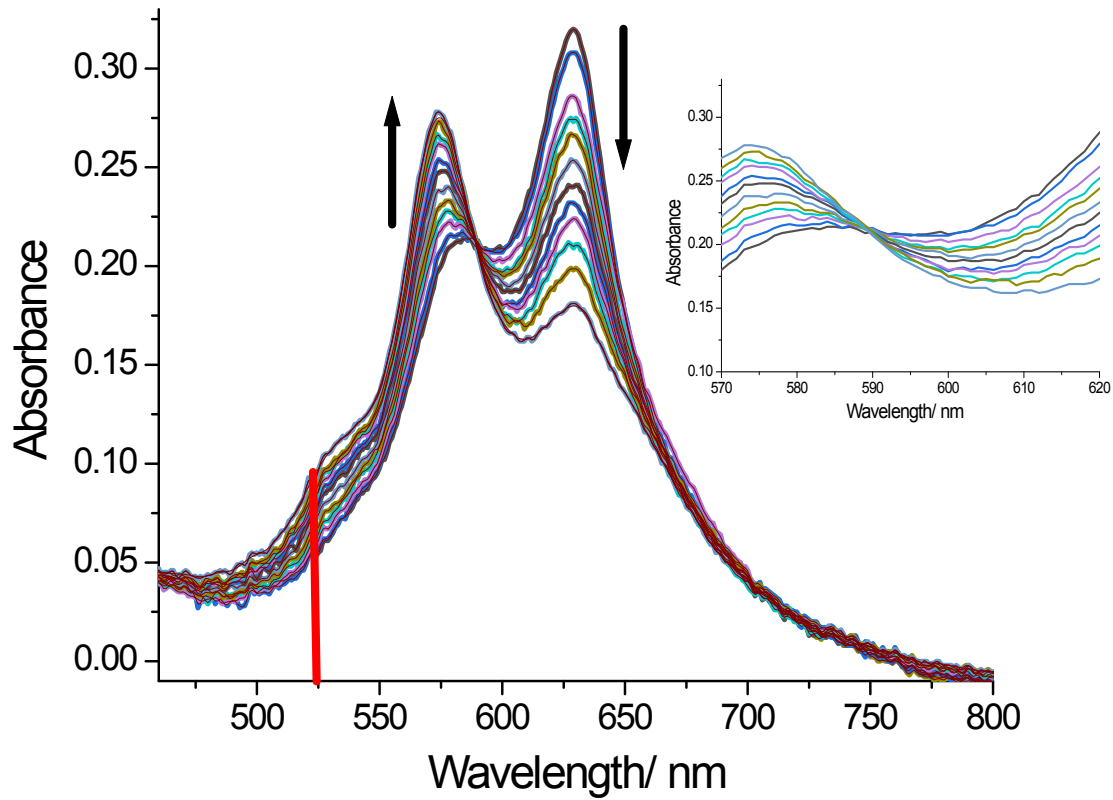


Figure S15. Changes to the absorption spectra for an aqueous solution of **OXJUL** (pH 7) after the addition of $\text{Na}_2\text{SO}_3(\text{aq})$ with the insert showing the isosbestic point. The red line indicates the excitation wavelength used for the fluorescence experiments and the slight increase in the optical density as the reaction proceeds.

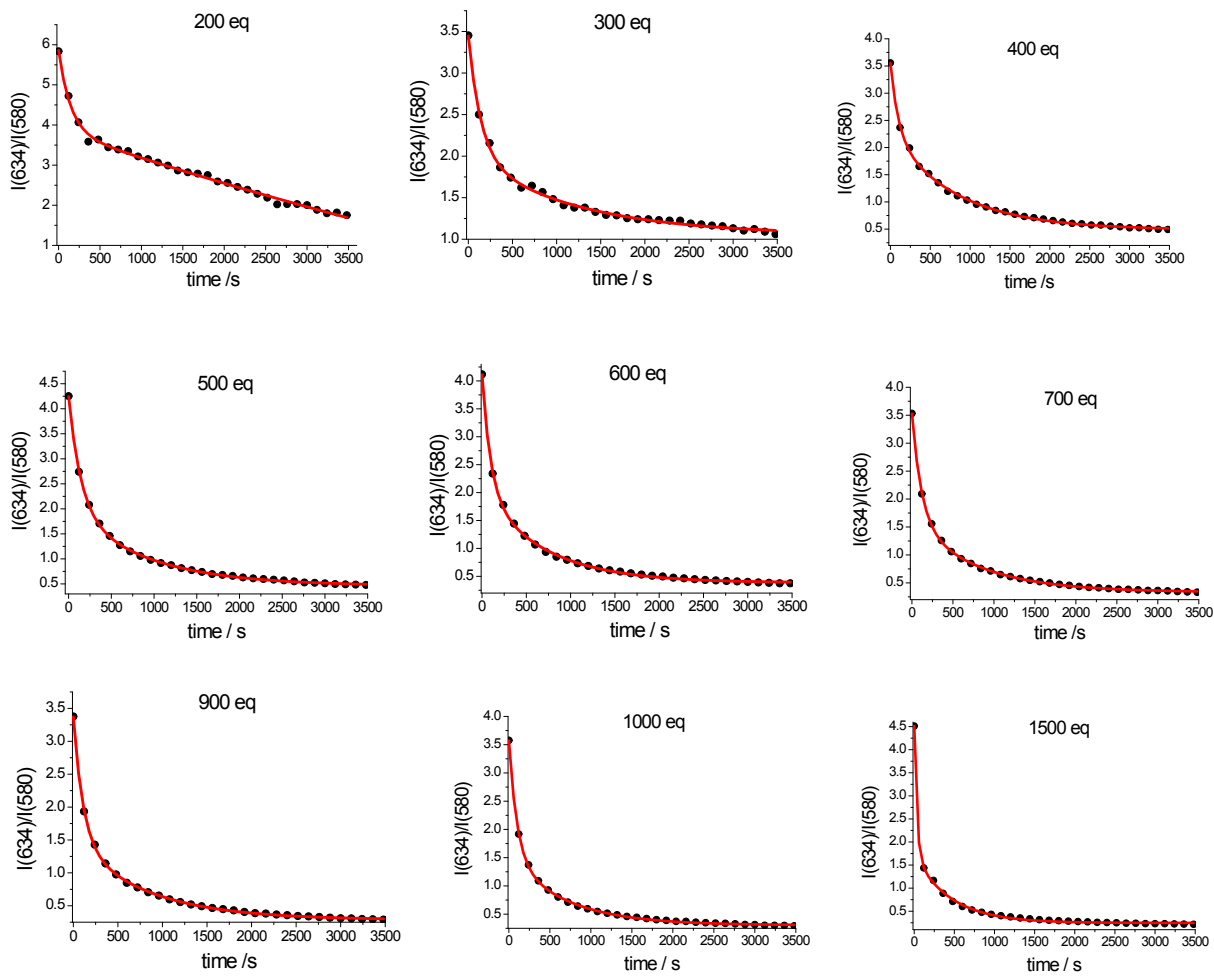


Table Calculated rate constant (k_1) obtained from fitting of the curves using two exponentials.

Equivalents SO_3^{2-}	$k_1 \cdot 10^{-3} \text{ s}^{-1}$
200	7.0
300	7.0
400	10.3
500	7.0
600	10.3
700	8.6
900	9.1
1000	10.1

Figure S16. Kinetic plots showing the alterations in $I(634)/I(580)$ versus time for several different equivalents of sulphite. Table of calculated rate constants.

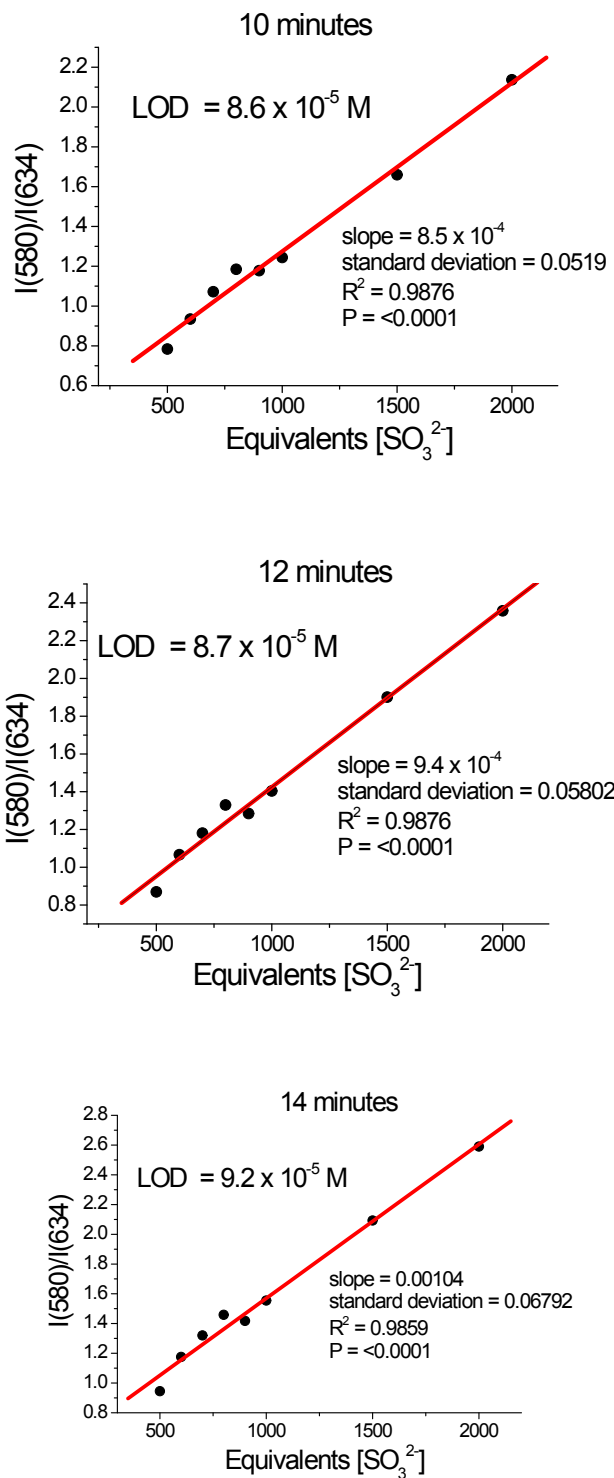


Figure S17. Calibration plots at various times for the detection of sulfite by OXJUL (conc = 0.47 μM).

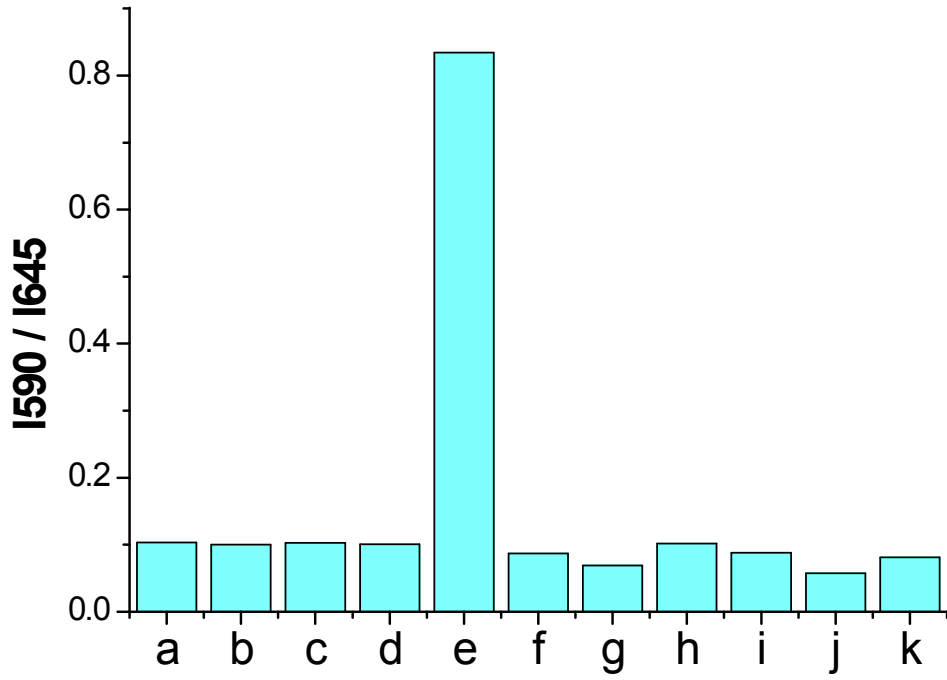


Figure S18. Anion selectivity comparison using the emission intensity ratio I_{590}/I_{645} for **OXJUL** upon addition of (a) F^- (b) Cl^- (c) Br^- (d) I^- (e) SO_3^{2-} (f) SO_4^{2-} (g) PO_4^{3-} (h) NO_3^- (i) NO_2^- (j) CO_3^{2-} (k) CH_3COO^- (3.9×10^{-4} mmol, $\lambda_{ex} = 525$ nm) in EtOH / H₂O (75 %, v/v).

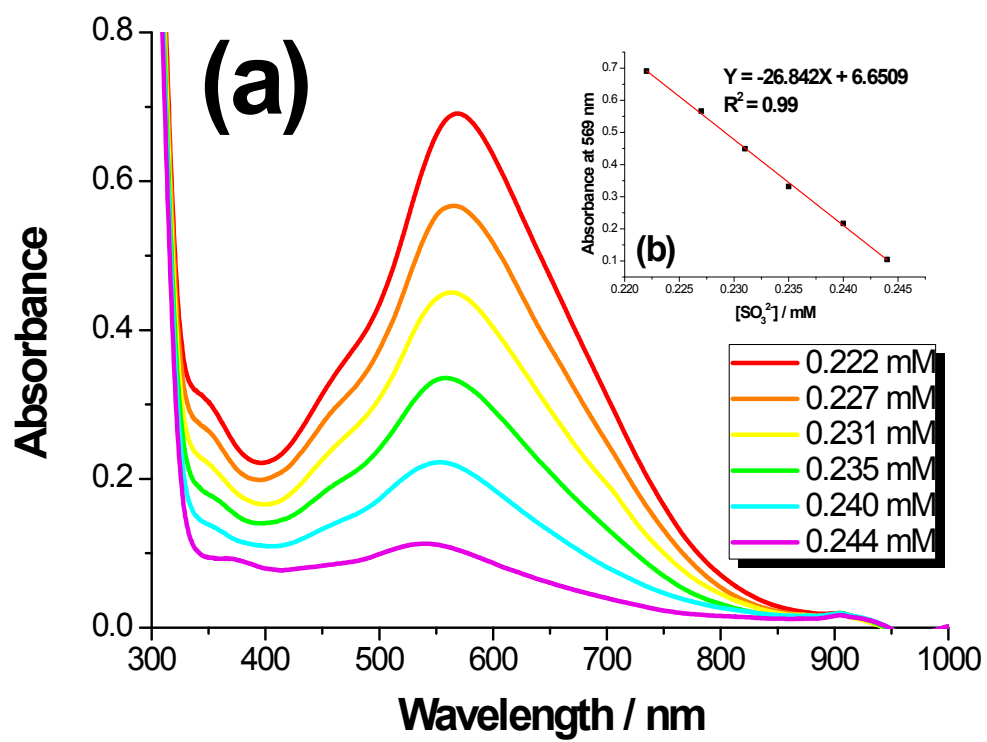


Figure S19. (a) UV-Vis absorption spectra of the iodometric measurement for sulfite detection upon different $[SO_3^{2-}]$ after reacting with I_2 . (b) The linear correlation plot for the UV-Vis absorption at 569 nm vs different $[SO_3^{2-}]$.

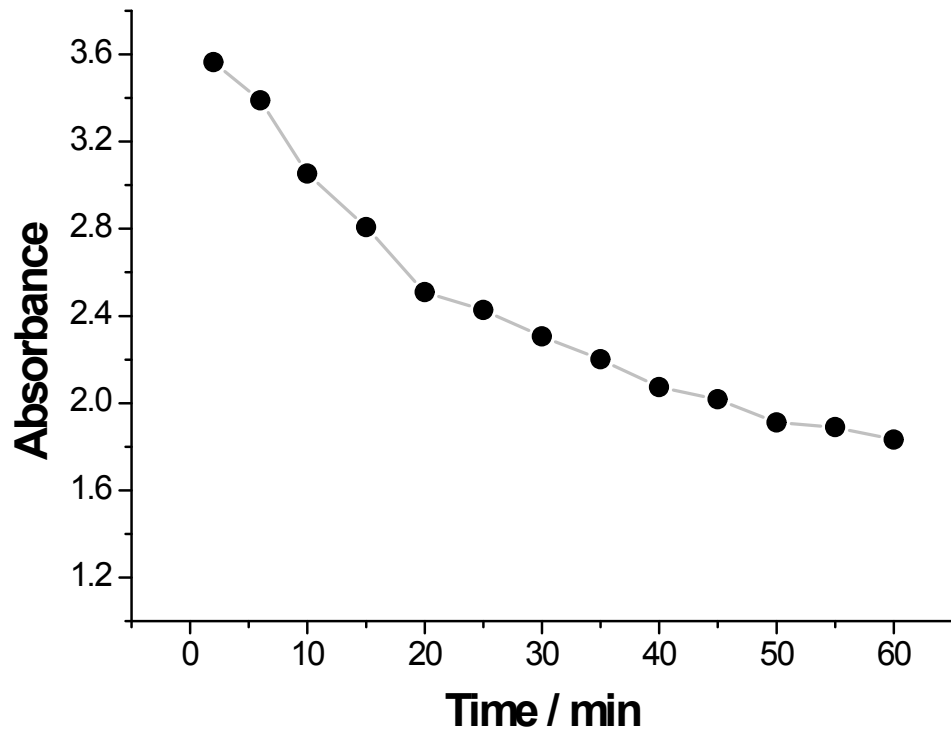


Figure S20. An example of UV-Vis absorbance changes during an iodometric measurement for a dry white wine sample.

Table S1. Crystal data and structure refinement for OXJUL

Empirical formula	C ₄₂ H _{43.25} BF ₂ N ₅ O ₈ S
Formula weight	826.93
Temperature/K	150.0(2)
Crystal system	triclinic
Space group	P-1
a/Å	8.04807(16)
b/Å	20.9106(6)
c/Å	25.9109(8)
α/°	109.598(3)
β/°	95.323(2)
γ/°	99.3812(19)
Volume/Å ³	4001.65(19)
Z	4
ρ _{calc} g/cm ³	1.373
μ/mm ⁻¹	1.310
F(000)	1733.0
Crystal size/mm ³	0.33 × 0.09 × 0.06
Radiation	CuKα ($\lambda = 1.54184$)
2Θ range for data collection/°	4.74 to 133.876
Index ranges	-6 ≤ h ≤ 9, -24 ≤ k ≤ 24, -30 ≤ l ≤ 30
Reflections collected	56540
Independent reflections	14171 [R _{int} = 0.0520, R _{sigma} = 0.0427]
Data/restraints/parameters	14171/949/1152
Goodness-of-fit on F ²	1.031
Final R indexes [I>=2σ (I)]	R ₁ = 0.0470, wR ₂ = 0.1177
Final R indexes [all data]	R ₁ = 0.0619, wR ₂ = 0.1289
Largest diff. peak/hole / e Å ⁻³	0.62/-0.41

Table S2. Results from DFT Calculations**JUL**

Calculation Method = RB3PW91

Basis Set = 6-311+G(d,p)

SCRF = IEFPCM, SOLVENT=DMSO

Charge = 0

Spin = Singlet

E(RB3PW91) = -1850.04100378 a.u.

RMS Gradient Norm = 0.00003228 a.u.

Imaginary Freq = 0

Dipole Moment = 22.8376 Debye

Point Group = C1

Final geometry:

Atom	Angstroms		
	x	y	z
F1	-2.289308	0.011399	1.144402
F2	-2.289308	-0.011401	-1.144398
N3	-0.553809	-1.246302	0.013402
N4	-0.553807	1.246298	-0.013398
N5	7.205592	-0.000008	0.000002
C6	1.287690	-2.541803	0.224402
H7	2.318790	-2.839904	0.331402
C8	0.179489	-3.364902	0.253502
H9	0.175688	-4.438402	0.367802
C10	-0.963110	-2.543102	0.126702
C11	-0.963107	2.543098	-0.126698
C12	0.179594	3.364898	-0.253498
H13	0.175695	4.438398	-0.367798
C14	1.287693	2.541797	-0.224398
H15	2.318794	2.839896	-0.331398
C16	1.548992	-0.000003	0.000002
C17	0.827393	1.214697	-0.055998

C18	0.827391	-1.214703	0.056002
C19	-2.353311	-2.913801	0.117202
H20	-3.061010	-2.098000	0.025702
C21	-2.799911	-4.185200	0.206302
H22	-2.079912	-4.994901	0.292302
C23	-4.195212	-4.602699	0.197302
C24	-4.503913	-5.968199	0.283602
H25	-3.712313	-6.707000	0.355302
C26	-5.830913	-6.376198	0.277302
H27	-6.072514	-7.434098	0.344002
N28	-6.866312	-5.535697	0.192902
C29	-6.573411	-4.231098	0.110602
H30	-7.420811	-3.553397	0.042902
C31	-5.284711	-3.721298	0.108602
H32	-5.143510	-2.649099	0.040202
C33	-2.353206	2.913799	-0.117198
H34	-3.061007	2.098000	-0.025698
C35	-2.799905	4.185200	-0.206298
H36	-2.079905	4.994899	-0.292298
C37	-4.195205	4.602701	-0.197298
C38	-4.503804	5.968201	-0.283598
H39	-3.712303	6.707000	-0.355298
C40	-5.830904	6.376202	-0.277298
H41	-6.072503	7.434102	-0.343998
N42	-6.866304	5.535803	-0.192998
C43	-6.573405	4.231102	-0.110598
H44	-7.420806	3.553403	-0.042898
C45	-5.284706	3.721302	-0.108598
H46	-5.143506	2.649101	-0.040198
C47	3.002792	-0.000005	0.000002
C48	3.737491	-0.887905	-0.808898
H49	3.206790	-1.555105	-1.480698
C50	5.117491	-0.903506	-0.827398
C51	5.842692	-0.000007	0.000002
C52	5.117492	0.903494	0.827402
C53	3.737492	0.887895	0.808902
H54	3.206793	1.555095	1.480702
C55	5.875690	-1.848707	-1.720798
H56	6.082190	-2.783107	-1.181898
H57	5.263790	-2.115606	-2.586698
C58	7.194591	-1.218208	-2.150298
H59	7.000591	-0.335907	-2.770198
H60	7.789090	-1.914008	-2.747498

C61	7.989591	-0.815408	-0.921898
H62	8.358290	-1.708208	-0.396398
H63	8.868491	-0.230709	-1.213098
C64	5.875693	1.848693	1.720802
H65	5.263793	2.115594	2.586702
H66	6.082194	2.783093	1.181902
C67	7.194593	1.218192	2.150302
H68	7.789093	1.913992	2.747502
H69	7.000592	0.335893	2.770202
C70	7.989592	0.815392	0.921902
H71	8.358293	1.708192	0.396402
H72	8.868492	0.230691	1.213102
B73	-1.465108	-0.000001	0.000002

OXJUL

Calculation Method = RB3PW91

Basis Set = 6-311+G(d,p)

SCRF = IEFPCM, SOLVENT=DMSO

Charge = 1

Spin = Singlet

E(RB3PW91) = -1848.06200066 a.u.

RMS Gradient Norm = 0.00000152 a.u.

Imaginary Freq = 0

Dipole Moment = 43.3070 Debye

Point Group = C1

Atom	Angstroms		
	x	y	z
F1	-2.256732	-0.021829	-1.159939
F2	-2.207584	0.025257	1.127595
N3	-0.492237	1.241330	-0.079153
N4	-0.504972	-1.257201	-0.026659

N5	7.242924	-0.001248	-0.086134
C6	1.375414	2.524747	-0.203018
H7	2.414614	2.811270	-0.262887
C8	0.281664	3.359276	-0.212610
H9	0.291424	4.436869	-0.272964
C10	-0.878495	2.544133	-0.136397
C11	-0.904165	-2.555131	0.046105
C12	0.248427	-3.384218	0.082964
H13	0.247356	-4.461803	0.144471
C14	1.350789	-2.563136	0.035437
H15	2.387920	-2.861220	0.061007
C16	1.581071	-0.020084	-0.089079
C17	0.877963	-1.227326	-0.041386
C18	0.889641	1.195193	-0.112255
C19	-2.261407	2.935938	-0.118424
H20	-2.984346	2.130255	-0.065144
C21	-2.678379	4.219673	-0.161302
H22	-1.939463	5.014915	-0.212763
C23	-4.063720	4.669786	-0.145063
C24	-4.336549	6.044051	-0.195018
H25	-3.526889	6.764598	-0.244378
C26	-5.653809	6.483499	-0.181526
H27	-5.870517	7.548027	-0.220276
N28	-6.707797	5.665095	-0.122638
C29	-6.448441	4.352061	-0.074382
H30	-7.312459	3.694237	-0.026515
C31	-5.172213	3.811206	-0.082555
H32	-5.056308	2.734662	-0.041050
C33	-2.291078	-2.930979	0.079817
H34	-3.006699	-2.117536	0.052390
C35	-2.719718	-4.210215	0.139972
H36	-1.987770	-5.013153	0.162561
C37	-4.109302	-4.645553	0.178500
C38	-4.394750	-6.017209	0.228316
H39	-3.591693	-6.746697	0.237390
C40	-5.716223	-6.442391	0.266784
H41	-5.942948	-7.504819	0.305564
N42	-6.762517	-5.612142	0.259623
C43	-6.491053	-4.301533	0.212254
H44	-7.349012	-3.634139	0.207403
C45	-5.209704	-3.774486	0.171236
H46	-5.083592	-2.698876	0.136210
C47	3.061830	-0.026524	-0.104131

C48	3.777564	0.591459	0.948139
H49	3.220888	1.039242	1.764687
C50	5.154156	0.621465	0.996241
C51	5.862664	0.004337	-0.062332
C52	5.167271	-0.633323	-1.127206
C53	3.755958	-0.635837	-1.125276
H54	3.233857	-1.107888	-1.949440
C55	5.887345	1.266821	2.138914
H56	5.978044	2.342605	1.944452
H57	5.302102	1.160627	3.054648
C58	7.272349	0.656673	2.298876
H59	7.200406	-0.378515	2.646510
H60	7.858491	1.210102	3.035089
C61	8.006388	0.705165	0.976011
H62	8.139834	1.736568	0.638127
H63	8.984045	0.229187	1.033595
C64	5.906835	-1.243082	-2.161872
H65	5.378822	-1.726279	-2.976561
C66	7.279594	-1.224526	-2.130354
H67	7.878893	-1.686375	-2.903204
C68	7.919687	-0.590212	-1.069435
H69	8.998807	-0.543090	-1.000240
B70	-1.415678	-0.002556	-0.033704